Heliyon 10 (2024) e39168

Contents lists available at ScienceDirect

Heliyon

journal homepage: www.cell.com/heliyon

Research article

Mixed bio-based surfactant-templated mesoporous silica for supporting palladium catalyst

Elianaso Elimbinzi [a,*], James E. Mgaya [b]

[a] Department of Chemistry, Mkwawa University College of Education, University of Dar es Salaam, Dar es Salaam, Tanzania
[b] Department of Chemistry, Dar es Salaam University College of Education, University of Dar es Salaam, Dar es Salaam, Tanzania

ARTICLE INFO

Keywords:
Catalyst
Cashew nut shell liquid
Palladium
Castor oil
Mesoporous silica

ABSTRACT

The study aimed on the synthesis of bio-based surfactant-templated mesoporous silica for supporting palladium catalyst using mixed bio-based templating agents namely cashew nut shell liquid (CNSL) and castor oil for pore direction purposes. The materials prepared through co-condensation of 3-aminopropyltriethoxysilane (APTS) and tetraethyl orthosilicate (TEOS) in a 1:4 M ratio using 1:1, 4:1 and 9:1 ratio of CNSL and castor oil. The resulting porous materials were utilized to support the palladium(II) chloride catalyst, resulting in a heterogeneous catalyst-a better and more environmentally friendly catalyst than a homogeneous one. Different instruments were used to characterize the prepared materials such as nitrogen porosimeter, Powder X-ray Diffraction, Diffuse Reflectance Infrared Fourier Transform Spectroscopy and Inductively coupled plasma optical emission spectroscopy. Physisorption studies of the prepared materials indicated that the largest pore diameter of 43.84 nm could be obtained by using a 1:1 M ratio of CNSL and castor oil. On the other hand, the largest surface area of 209 m^2/g was obtained from a 9:1 whereas the largest pore volume was 1.55 cm^3/g from a 4:1. Diffuse Reflectance Infrared Fourier Transform Spectroscopy analysis confirmed the presence of N-H group, the bending vibration bands at around 1640 and 1543 cm^{-1} indicating that the reaction of organoaminesilanes and tetraethyl orthosilicate had occurred. The palladium content of the supported catalyst was determined by ICP-OES which confirmed the attachment of palladium to the synthesized materials. The highest palladium loading was obtained from the adsorbent prepared by using 1:1 ratio of surfactants mixture which gave the adsorption value of 2.16 mmol/g. Powder X-ray Diffraction indicated that the synthesized organosilica materials are amorphous with improved crystallinity upon attachment of palladium catalyst. The incorporation of palladium in the synthesized materials using the mixed bio-based surfactant was successful.

1. Introduction

Researchers are interested in mesoporous materials having ordered pores because of their many uses in medication delivery, adsorption, catalysis, separation technology, and polymer reinforcing agents. They can also be used as supports for immobilizing biomolecules [1–11]. Pore directing agent used during the synthesis of mesoporous material can be done through two methods: hard-templating and soft-templating [12]. The hard-templating method pre-synthesized mesoporous solids or colloidal crystals are

* Corresponding author.
E-mail addresses: elianaso.kimambo@muce.ac.tz, eelianaso@yahoo.com (E. Elimbinzi).

https://doi.org/10.1016/j.heliyon.2024.e39168
Received 17 October 2023; Received in revised form 8 August 2024; Accepted 8 October 2024
Available online 10 October 2024

used as a sacrificial mold to prepare the desired materials [13]. The soft-templating method, on the other hand, uses micelles, which are typically composed of amphiphilic surfactants and block copolymers, as a source of templates [14]. These micelles form ordered mesostructures when combined with organic or inorganic precursors [15]. Contrary to the hard-templating method, the micelles derived from amphiphilic surfactants and block copolymers are tunable to regulate mesostructures in order to suit the intended applications. One of the approaches used to regulate mesostructures is the use of surfactants mixture instead of single surfactant as the source of templates to produce mesoporous materials with improved properties [16–21]. The improved properties are a result of synergistic behaviour of surfactants mixtures arising from favorable forces acting between surfactants [22]. A study done by Kobayashi et al. [23] on the synthesis of mesoporous materials using a mixture of cetyltrimethylammonium bromide (CTAB) and cetylpyridinium bromide (CPB) surfactants indicates that the two surfactants co-exist in the pores without forming significant monocomponent domain structures. Various surfactant mixtures have been reported so far as suitable sources of templates which include; cationic and nonionic surfactants, anionic and nonionic surfactants, two cationic surfactants, and two nonionic surfactants mixtures [19,24,25]. For instance, it has been reported that mixtures of the cationic surfactant CTAB and the nonionic Pluronic P123 produce structurally stable MCM-48 mesoporous silica with an extremely low surfactant to silica source molar ratio [26]. The MCM-48 prepared by using mixed surfactants shows higher adsorption of vitamin B12 than materials prepared by using the single cationic CTAB template [26]. Nonionic block copolymer P123 (EO20PO70EO20) and anionic sodium dodecyl sulphate mixtures have also been reported in the preparation of mesoporous silica with high surface area (770 m^2/g), large pore volume (1.5 cm^3/g), and uniform pore size (10 nm) [27]. Prolonged hydrothermal treatment had no effect on cell parameters of the prepared materials indicating that the materials have excellent thermal stability. Similarly, using mixed anionic surfactants; sodium dodecyl benzene sulfonate and sodium dodecyl sulphate as templates, large pore mesoporous silica with uniform size and pore diameters up to 10.3 nm was produced [19]. Interestingly, mesopores could not form when sodium dodecyl benzene sulfonate or sodium dodecyl sulphate were used separately in the synthetic procedure. These bio-based surfactants have been separately used before as sources of templates to produce mesoporous materials suitable for adsorption, immobilization of biomolecules and catalysis purposes [28–32]. Based on the synergistic effects of binary systems reported for several surfactant mixtures, this study investigated the structural properties of mesoporous materials prepared using mixtures of cashew nut shell liquid (CNSL) and castor oil surfactants presented in Figs. 1 and 2. Using of bio surfactant add value to the environment as they are biodegradable and environmentally friend. In addition, the cashew nut shells in Tanzania are thrown out as the waste, using them for research reduce the wastes in the environment. The study will contribute knowledge towards replacement of potentially toxic chemicals with environmentally friendly materials also contribute circular economy. Also, the incorporation of palladium(II) chloride into mesoporous support add value to the homogenous palladium(II) chloride [33] and turn to heterogenous catalyst. The heterogenous catalyst is easier in separation compared to the homogeneous catalyst [34]. Palladium supported materials has been reported to have various application such as electrocatalysis, can be used in sensors, fuel cells, biomedical (photothermal therapy, anticancer treatment, antibacterial) and hydrogen storage [35–38].

2. Materials and methods

2.1. Materials and reagents

Cashew nut shells and castor oil beans were collected from Coastal and Iringa regions of Tanzania, respectively. Chemicals; tetraethyl orthosilicate (TEOS, 98%), 3-aminopropyltriethoxysilane (APTS, >97%), ethanol (98%), petroleum ether (40–60 °C), palladium(II) chloride (99%), 2-quinoline carboxaldehyde (97%), *n*-hexane and potassium bromide (99 %). All chemicals were bought from Sigma Aldrich and used without further purification. CNSL and castor oil were obtained by the solvent extraction methods reported earlier [29,30].

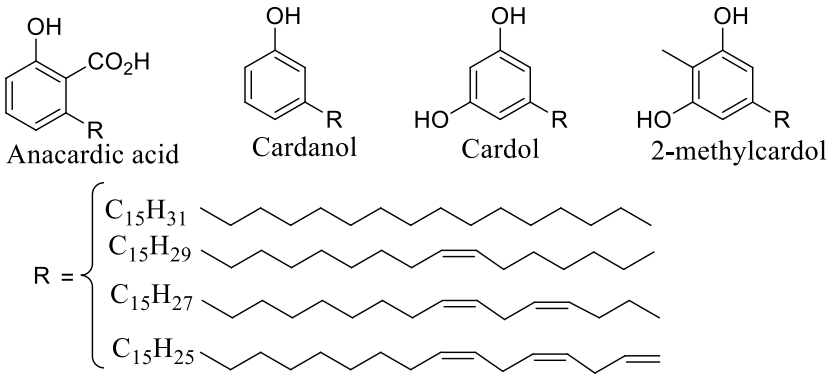

Fig. 1. Components of cashew nut shell liquid.

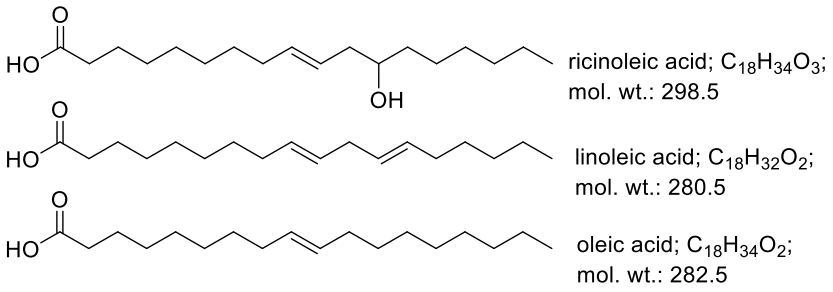

Fig. 2. Major components of castor oil fatty acids.

2.2. Synthesis of organically modified micelle templated silica

Using mixture of CNSL and castor oil surfactants in various ratios (CNSL: castor oil); 1:0, 0:1, 1:1, 4:1, and 9:1, the organically modified micelle templated silica (MTS-APTS) samples were synthesized using the co-condensation method. Aqueous ethanol (46 mL pure ethanol and 53 mL distilled water) containing 2.50 g of CNSL/castor oil was mixed at 25 °C and atmospheric pressure. Then TEOS (8.3 g) and APTS (1.90 g) were added separately but simultaneously and rapidly while stirring. The reaction was kept for 24 h at 40 °C. The resulting mixture was filtered to obtain a wet solid, which was subsequently subjected to Soxhlet extraction for 10 h with ethanol to remove the template. The obtained surfactant-free solid (MTS-APTS) was dried in an oven at 100 °C for 8 h before stored in clean, sealed bottles in desiccators for further modifications and characterization.

2.3. Attachment of 2-quinoline carboxaldehyde ligand to modified micelle template silica

MTS-APTS (2.01 g) was slowly added to a stirred mixture of 2-quinoline carboxaldehyde (1.16 g) and absolute ethanol (50 mL), and the mixture was refluxed at 60 °C and vigorously stirred for 10 h. The resulting product mixture was filtered under low pressure to obtain the solid (MTS-APTS-L), which was then washed with excess ethanol and dried in a 100 °C oven. When the quinoline carboxaldehyde ligand attached to the modified mesoporous silica the quinoline-2-carboimine resulted. Similar procedure was used to prepare materials using different surfactant ratios. The dried samples were stored in desiccators for characterization and also was used for supporting of palladium catalyst.

2.4. Preparation of supported palladium catalyst

The MTS-APTS-supported Pd catalyst MTS-APTS-L-Pd) was prepared by mixing the ligand-modified silica (1.50 g) with the solution of palladium(II) chloride (0.05 g) in absolute ethanol in the round bottom flask under reflux for 5 h at 60 °C. The resulting supported palladium catalyst was filtered and thoroughly washed with absolute ethanol until the washings were colorless before being dried overnight in the oven at 100 °C. The general scheme for preparation of mesoporous silica supported palladium is summarized in Fig. 3. The MTS-APTS was needed in order to attach the ligand and then the lone pair from the amine and quinoline-2-carboimine attached to

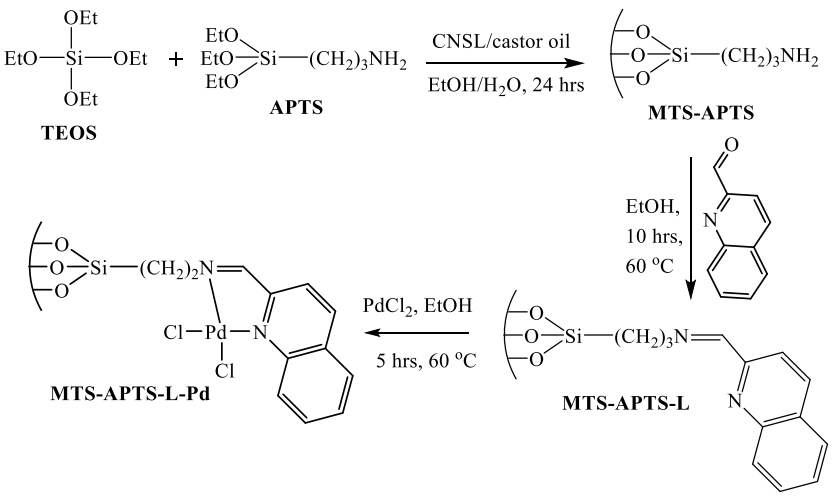

Fig. 3. General scheme for preparation of mesoporous silica supported palladium.

the MTS were used to incorporate of palladium in the materials.

2.5. Characterization of the synthesized mesoporous materials and supported palladium catalyst

N_2 porosimetry at 77 K, was carried out using a Quantachrome instrument (Nova 4200 multi-station nitrogen sorption). The specific surface area was calculated from the adsorption data using the Brunauer-Emmett-Teller (BET) method for P/Po values between 0.05 and 0.3, and the pore size distribution of porous materials was calculated using the Barrett-Joyner-Halenda (BJH) method from the desorption branches of the isotherm [39–41]. Prior to physisorption studies, samples were dried overnight at 120 °C and evacuated for 3 h to remove physisorbed molecules and avoid any drastic change due to surface modification [41].

Diffuse reflectance infrared Fourier transform spectroscopy (DRIFTS, PerkinElmer 2000 spectrophotometer) was used to identify the functional groups present in the synthesized materials. Samples for DRIFT analysis were mixed with potassium bromide (KBr) in a 9:1 (w/w ratio), grounded by using a mortar and pestle and dried overnight in an oven at 80 °C. The diluted, dried, finely ground sample was then placed in a cup disc for analysis. Each spectrum was typically acquired with 64 scans at a resolution of 4 cm^{-1}. The absorbance and wave numbers 4 cm^{-1}. The final spectra were obtained by subtracting the KBr background spectrum from the sample spectra and were reported in absorbance and wave numbers (cm^{-1}).

X-ray powder diffraction (XRD) spectra were recorded using CuKα radiation (λ = 0.1542 nm) and 2θ sampling technique. The voltage was set to 40 kV and the current to 40 mA. The scan was performed between 5 and 85° with a step size of 0.07°. The time per step was set at 10 s and the analysis took 3 h per sample. Samples for XRD analysis were not weighed but care was taken to ensure that they were of similar size so that the peak intensities could be compared.

Inductively Coupled Plasma-Optical Emission Spectroscopy (ICP-OES) was used to determine the palladium content in the catalyst samples prepared by using different ratios of CNSL/castor surfactant mixture. Prior to analysis, supported Pd catalyst sample (0.20 g) was digested in aqua regia for an hour in order to obtain the palladium solution from the silica supports. The mixture was then diluted with distilled water to 250 mL. The supernatant from the dilute solution was then used for ICP-OES analysis.

3. Results and discussion

3.1. Nitrogen adsorption-desorption isotherms

Physisorption studies were carried out to investigate the porous nature of the synthesized materials. The characteristics of the synthetic materials are shown by the adsorption-desorption isotherms. The adsorption and desorption processes that typically take place in mesoporous materials led to the creation of hysteresis loops in several synthetic samples. A feature of mesoporous material, type IV adsorption-desorption isotherms was displayed by the produced micelle template silica. Several samples produced by altering the surfactant ratios revealed an enormous rise at 0.9 (P/Po), where the adsorption rate was high with the formation of hysteresis loop. Fig. 4 (a) shows the N_2 adsorption-desorption isotherms of MTS-APTS materials synthesized by using different surfactant ratios. Type IV adsorption isotherm was observed for the synthesized materials which is typical of mesoporous characteristic based on the IUPAC classification [42]. Samples made from 1:1 and 4:1 surfactant mixtures adsorb at slightly higher P/P_O values than those made from single surfactants, 1:0, 0:1. This indicates that templates derived from 1:1 and 4:1 surfactant mixtures produced materials with relatively larger pore sizes compared to those made by using single surfactant. But then, surfactant ratio of 9:1 resulted into materials which adsorbs at smaller P/P_O value than those made from single surfactant. Fig. 4 (b) shows the isotherms of selected samples using 4:1 surfactant mixture before and after the palladium loading. The P/P_O value of the supported catalyst (MTS-APTS-L-Pd) shifted to a slightly lower value compared to MTS-APTS which suggests that the accessible pore size of mesoporous materials slightly decreases upon introduction of palladium. Generally, immobilization of palladium on mesoporous materials had no effect on the type of isotherms which maintained type IV before and after respective modifications. The synthesized materials possess the characteristics of mesoporous materials as compared to other mesoporous materials prepared using artificial surfactants [43,44]. However, the BET surface area is observed to be low compared to the reported by other researchers as in this study the higher BET surface area was 211

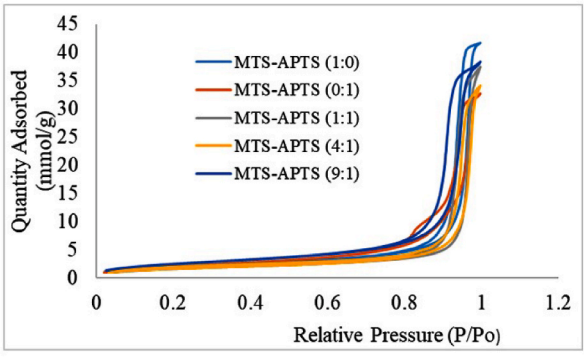

Fig. 4a. Adsorption-desorption isotherms of mesoporous silica from different surfactant mixture ratios.

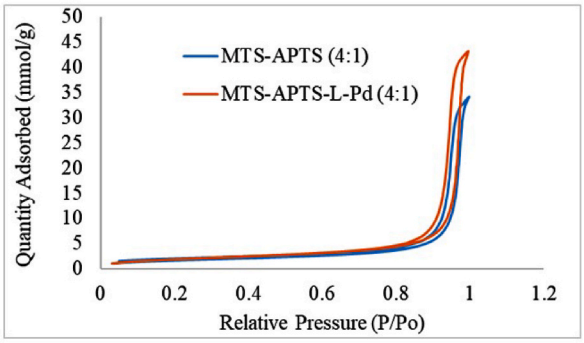

Fig. 4b. Adsorption-desorption isotherms of MTS-APTS (4:1) and MTS-APTS-L-Pd (4:1).

m^2/g [16,27,43,45].

The Barrett-Joyner-Halenda (BJH) pore size distribution was determined from the desorption branch and is presented in Fig. 5 (a). The synthesized materials have generally wide pore size distribution with broad peaks centred at around 39, 38, 44, 41 and 29 nm, corresponding to the mesoporous prepared by using 1:0. 0:1, 1:1, 4:1 and 9:1 surfactant mixture, respectively.

Loading of palladium to MTS-APTS had negligible effect on the pore size distribution of the materials as shown in a selected sample (4:1), Fig. 5 (b)

Table 1 summarizes the average pore diameter, BET surface areas, and total pore volume obtained from N_2 adsorption-desorption measurements. Results reveal that samples prepared using from surfactant mixtures (1:1 and 4:1) have larger pore sizes than those made from single surfactant. Diverse observation seems for 9:1 material in which the pore size measured is lesser related to single surfactant synthesized mesoporous materials. Large sized pores are usually desirable for immobilization of metal complexes as well as diffusion of larger molecules [46,47]. The pore diameter of these synthesized materials range from 25 nm to 43 nm which is large compared to other synthesized material using bio surfactant [30,45]. Having materials with large pore is of advantages as its support the kinetic of immobilized catalyst and increase its catalytic activities [48,49].

3.2. Amount of palladium incorporated into mesoporous silica materials

The palladium content of the supported catalyst was analyzed by ICP-OES and the results are summarized in Table 2. Findings reveal that materials with relatively larger pore sizes have slightly higher loadings and vice versa in agreement with previous studies [50], where the proportion of gold nanoparticles incorporated into mesoporous silica nanoparticles increased with the increasing pore sizes of the mesoporous materials. The observed increase in adsorbed metal species with increasing pore size is due to a reduced geometric barrier for metals penetrating the mesoporous silica matrix.

3.3. Powder X-ray diffraction

Powder X-ray diffraction was used to study the architecture of the pores of the materials. There was no observable difference in XRD patterns of samples made by using different surfactant ratios. XRD spectra for the MTS-APTS and MTS-APTS-L, Fig. 6a and b showed a broad diffraction peaks around 2Θ; 25° and 10° suggesting that the pore structures are surrounded by amorphous walls [51]. Attachment of palladium to the MTS-APTS-L, the peaks appear around 2Θ 40°, 45°, 65°, 84° as shown in Fig. 6a, b and 6c for 1:0, 1:1

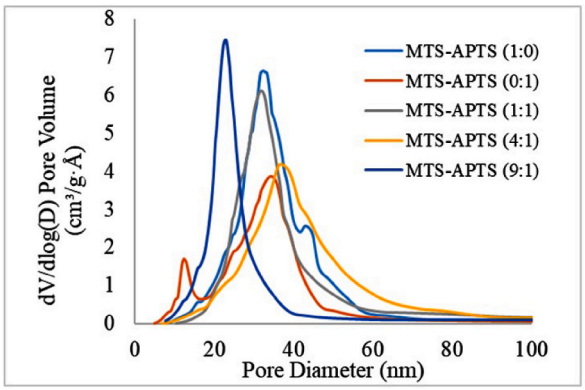

Fig. 5a. Pore size distribution of mesoporous silica from different surfactant ratios.

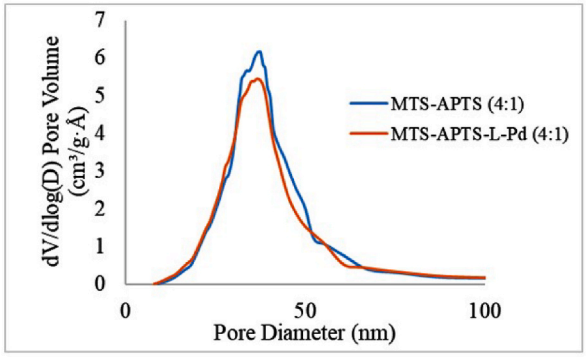

Fig. 5b. Pore size distribution of MTS-APTS (4:1) and MTS-APTS-L-Pd (4:1).

Table 1
Textural properties of the mesoporous silica materials (MTS-APTS, MTS-APTS-L, MTS-APTS-L-Pd).

Material	Ratios (CNSL: castor oil)	Average pore diameter (nm)	BET surface area (m^2/g)	Total pore volume (cm^3/g)
MTS-APTS	0:1	38.1720	211.2709	1.903931
MTS-APTS	1:0	39.0341	164.2834	1.460763
MTS-APTS	1:1	43.8409	135.7435	1.479458
MTS-APTS-L	1:1	41.7547	131.3398	1.29659
MTS-APTS-L-Pd	1:1	25.4695	120.1842	0.699292
MTS-APTS	4:1	41.1906	160.6500	1.554285
MTS-APTS-L	4:1	40.0094	145.1406	1.48868
MTS-APTS-L-Pd	4:1	37.4389	135.6187	1.168516
MTS-APTS	9:1	29.1828	207.9838	1.521464

Table 2
Palladium loading on synthesized supports.

MTS materials (CNSL:CO)	Average pore size (nm)	Loading of Pd^{2+} (mmol/g)
MTS-APTS-L(1:1)	41.755	2.157
MTS-APTS-L(4:1)	40.001	1.961
MTS-APTS-L(9:1)	25.507	1.605

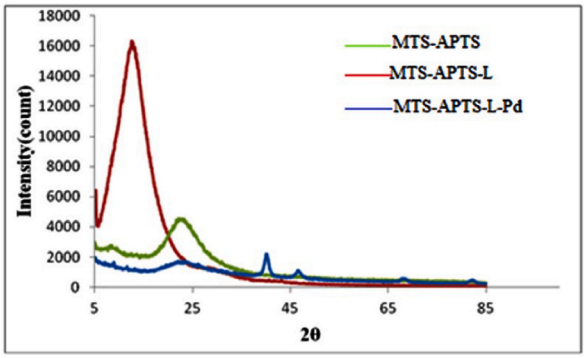

Fig. 6a. XRD spectra for MTS-APTS, MTS-APTS-L and MTS-APTS-L-Pd made with 1:0 surfactant ratio.

and 4:1 surfactant ratio used however, the peaks are not seen well when 4:1 was used to synthesize materials. The improvement of crystallinity of the synthesized mesoporous materials could possibly due to the addition of palladium species [52]. Peaks formation on MTS-APTS, MTS-APTS-L and MTS-APTS-L-Pd differed as the variation of surfactant ratios as shown in Fig. 6a, b, and 6c. This suggested that the changing the surfactant ratios has influence on the synthesized mesoporous materials. It is observed that changing surfactant ratio during the synthesis of the materials resulted into different XRD patterns, for instance, the XRD patterns for 1:1 was different from the 4:1 surfactant used as shown in Fig. 6b and c respectively.

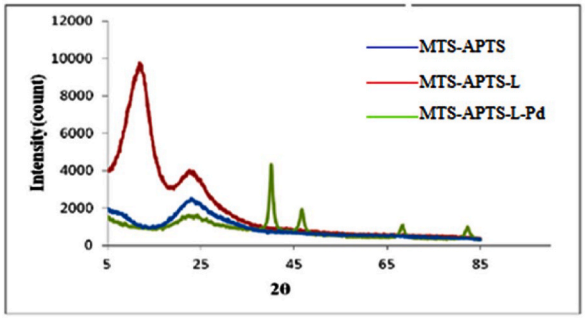

Fig. 6b. XRD spectra for MTS-APTS, MTS-APTS-L and MTS-APTS-L-Pd made with 1:1 surfactant ratio

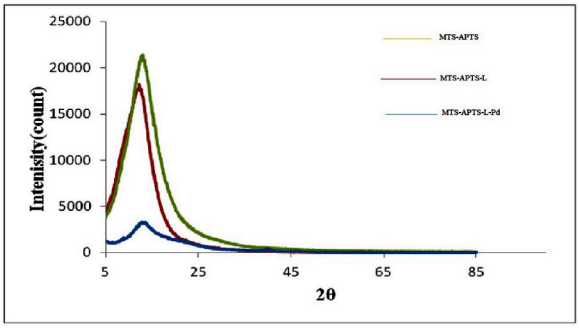

Fig. 6c. XRD spectra for MTS-APTS, MTS-APTS-L and MTS-APTS-L-Pd synthesized using 4:1 surfactant ratio.

3.4. DRIFTS of MTS-APTS, MTS-APTS-L, MTS-APTS-L-Pd materials

DRIFT analysis was executed to determine the type of functional groups present in the prepared materials. FT-IR spectra of materials made by using different surfactant ratios basically appeared to be similar and contained all expected functional groups. Fig. 7 (a) and 7 (b) show the FT-IR spectra of selected samples (4:1 and 1:1) for both unmodified (MTS-APTS), ligand modified (MTS-APTS-L) and palladium supported (MTS-APTS-L-Pd) materials in in the range 500–4000 cm^{-1}. The spectrum for MTS-APTS contains two peaks at 1640 cm^{-1} and 1543 cm^{-1} which correspond to N-H bending vibration. Spectra for MTS-APTS-L and MTS-APTS-L-Pd contain the stretching bands at 1690-1640 cm^{-1} for C=N and 1342-1266 cm^{-1} for C-N in the aromatic amine of the ligand. The MTS-APTS-L-Pd spectrum also contains a peak at 950 cm^{-1} which is assigned to Pd-N group. Other regions of the spectra were observed for both modified and unmodified materials such as the peaks at 3600–3000 cm^{-1} region assigned to the silanol OH groups and 1250-1020 cm^{-1} attributed to C-N stretching vibration band. Typical Si-O-Si- stretching vibration bands at 790 and 1110 cm^{-1}, which are attributed to the formation of a condensed silica network were also observed. In addition, there noisy around 4000-2700 cm^{-1} which could be due to the organic materials used during the preparation of palladium supported materials.

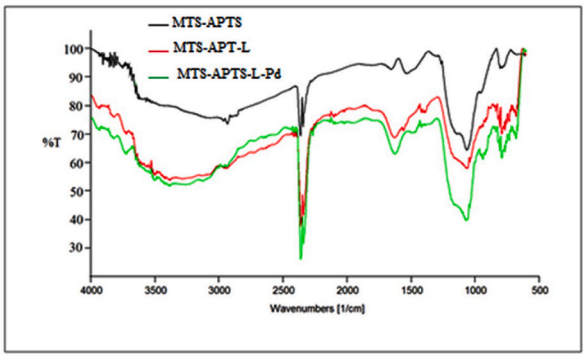

Fig. 7a. The IR spectra for the MTS-APTS, MTS-APTS-L and MTS-APTS-L-Pd prepared using 1:1 surfactant ratio.

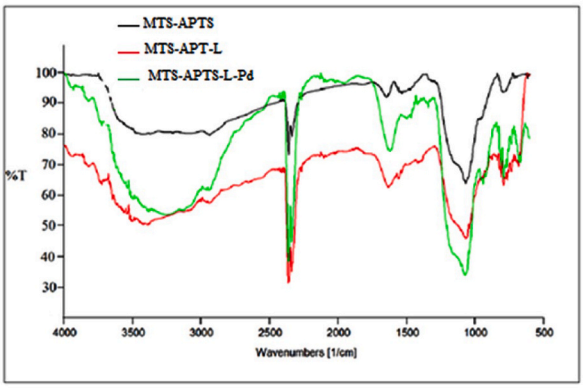

Fig. 7b. The IR spectra for the MTS-APTS, MTS-APTS-L and MTS-APTS-L-Pd prepared using 4:1 surfactant ratio.

4. Conclusion

The use of CNSL and castor oil mixtures in different proportions as templates for the synthesis of amine-functionalized mesoporous silica materials was successful. The synthesized material was used as the support for the palladium catalyst. The prepared materials were characterized as amorphous, with pore diameters of up to 43 nm, which is larger than that reported for single surfactants upon attachment of palladium into the material the crystallinity properties improved. Immobilization of palladium catalyst onto the amine functionalized samples was successful as confirmed by ICP-OES and DRIFT analysis.

CRediT authorship contribution statement

Elianaso Elimbinzi: Writing – original draft, Resources, Methodology, Investigation, Formal analysis, Data curation, Conceptualization. **James E. Mgaya:** Writing – review & editing, Validation.

Declaration of competing interest

The authors declare that they have no known competing financial interests or personal relationships that could have appeared to influence the work reported in this paper.

Acknowledgement

Authors are thankful to Mkwawa University College of Education (MUCE) for financial support.

References

[1] Y. Miyake, M. Hanaeda, M. Asada, Separation of organic compounds by spherical mesoporous silica prepared from W/O microemulsions of tetrabutoxysilane, Ind. Eng. Chem. Res. 46 (2007) 8152–8157, https://doi.org/10.1021/ie0705047.
[2] G. Zhao, B. Aziz, N. Hedin, Carbon dioxide adsorption on mesoporous silica surfaces containing amine-like motifs, Appl. Energy 87 (2010) 2907–2913, https://doi.org/10.1016/j.apenergy.2009.06.008.
[3] A.-M. Putz, O.I. Ivankov, A.I. Kuklin, V. Ryukhtin, C. Ianăşi, M. Ciopec, A. Negrea, L. Trif, Z.E. Horváth, L. Almásy, Ordered mesoporous silica prepared in different solvent conditions: application for Cu(II) and Pb(II) adsorption, Gels 8 (2022) 443, https://doi.org/10.3390/gels8070443.
[4] V. Hernández-Morales, R. Nava, Y.J. Acosta-Silva, S.A. Macías-Sánchez, J.J. Pérez-Bueno, B. Pawelec, Adsorption of lead (II) on SBA-15 mesoporous molecular sieve functionalized with -NH2 groups, Microporous Mesoporous Mater. 160 (2012) 133–142, https://doi.org/10.1016/j.micromeso.2012.05.004.
[5] C. Wu, F. Guo, L. Zhuang, X. Ai, F. Zhong, H. Yang, J. Qian, Mesoporous silica reinforced hybrid polymer artificial layer for high-energy and long-cycling lithium metal batteries, ACS Energy Lett. 5 (2020) 1644–1652, https://doi.org/10.1021/acsenergylett.0c00804.
[6] J.A.S. Costa, R.A. De Jesus, D.O. Santos, J.B. Neris, R.T. Figueiredo, C.M. Paranhos, Synthesis, functionalization, and environmental application of silica-based mesoporous materials of the M41S and SBA-n families: a review, J. Environ. Chem. Eng. 9 (2021), https://doi.org/10.1016/j.jece.2021.105259.
[7] S. He, H. Pan, J. Zhang, Advances of typical mesoporous materials and the application in drug delivery, Mater. Res. Express 10 (2023), https://doi.org/10.1088/2053-1591/acc82d.
[8] C. Zhang, H. Xie, Z. Zhang, B. Wen, H. Cao, Y. Bai, Q. Che, J. Guo, Z. Su, Applications and biocompatibility of mesoporous silica nanocarriers in the field of medicine, Front. Pharmacol. 13 (2022) 1–18, https://doi.org/10.3389/fphar.2022.829796.
[9] C. Bharti, N. Gulati, U. Nagaich, A. Pal, Mesoporous silica nanoparticles in target drug delivery system: a review, Int. J. Pharm. Investig. 5 (2015) 124–133, https://doi.org/10.4103/2230-973X.160844.
[10] C. Ianăşi, N.S. Nemeş, B. Pascu, R. Lazău, A. Negrea, P. Negrea, N. Duteanu, M. Ciopec, J. Plocek, P. Alexandru, B. Bădescu, D.M. Duda-Seiman, D. Muntean, Synthesis, characterization and antimicrobial activity of multiple morphologies of gold/platinum doped bismuth oxide nanostructures, Int. J. Mol. Sci. 24 (2023), https://doi.org/10.3390/ijms241713173.
[11] G. Mladin, M. Ciopec, A. Negrea, N. Duteanu, P. Negrea, P. Svera, m. Ianăşi, C. Ianăşi, Selenite removal from aqueous solution using silica–iron oxide nanocomposite adsorbents, Gels 9 (2023) 497, https://doi.org/10.3390/gels9060497.
[12] Y. Xie, D. Kocaefe, C. Chen, Y. Kocaefe, Review of research on template methods in preparation of nanomaterials, J. Nanomater. 2016 (2016), https://doi.org/10.1155/2016/2302595.

[13] S.M. Savić, K. Vojisavljević, M.P. Nešić, K. Živojević, M. Mladenović, N.Ž. Knežević, S. Savic, K. Vojisavljevic, M. Počuča-Nešić, K. Zivojevic, M. Mladenovic, N. Knezevic, Hard template synthesis of nanomaterials based on mesoporous silica, Metall. Mater. Eng. 24 (2018), https://doi.org/10.30544/400.
[14] H. Qutaish, S. Tanaka, Y.V. Kaneti, J. Lin, Y. Bando, A.A. Alshehri, S.I. Yusa, Y. Yamauchi, M.S.A. Hossain, J. Kim, Soft-templated synthesis of mesoporous nickel oxide using poly(styrene-block-acrylic acid-block-ethylene glycol) block copolymers, Microporous Mesoporous Mater. 271 (2018) 16–22, https://doi.org/10.1016/j.micromeso.2018.05.015.
[15] T. Zhao, A. Elzatahry, X. Li, D. Zhao, Single-micelle-directed synthesis of mesoporous materials, Nat. Rev. Mater. 4 (2019) 775–791, https://doi.org/10.1038/s41578-019-0144-x.
[16] L. Cao, J.G. Shao, Y.B. Yang, Y.X. Yang, X.N. Liu, Synthesis of mesoporous silica with cationic-anionic surfactants, Glas. Phys. Chem. 36 (2010) 182–189, https://doi.org/10.1134/S1087659610020069.
[17] H. Lin, F. Qu, X. Wu, M. Xue, G. Zhu, S. Qiu, Mixed surfactants-directed the mesoporous silica materials with various morphologies and structures, J. Solid State Chem. 184 (2011) 1415–1420, https://doi.org/10.1016/j.jssc.2011.03.043.
[18] H.H. Park, T.J. Ha, H.G. Im, S.J. Yoon, H.W. Jang, Pore structure control of ordered mesoporous silica film using mixed surfactants, J. Nanomater. 2011 (2011), https://doi.org/10.1155/2011/326472.
[19] F. Gai, T. Zhou, G. Chu, Y. Li, Y. Liu, Q. Huo, F. Akhtar, Mixed anionic surfactant-templated mesoporous silica nanoparticles for fluorescence detection of Fe^{3+}, Dalton Trans. 45 (2016) 508–514, https://doi.org/10.1039/c5dt03052h.
[20] H. Teng, T. Shen, Y. Hou, Y. Chen, X. Kou, X. Wang, M. Hai, Effect of salts on synthesis of mesoporous materials with mixed cationic and anionic surfactants as templates, Colloid J. 78 (2016) 690–697, https://doi.org/10.1134/S1061933X16050203.
[21] S. Das, E.D. Oldham, H.J. Lehmler, B.L. Knutson, S.E. Rankin, Tuning the position of head groups by surfactant design in mixed micelles of cationic and carbohydrate surfactants, J. Colloid Interface Sci. 512 (2018) 428–438, https://doi.org/10.1016/J.JCIS.2017.10.066.
[22] S. Kumar Shah, G. Chakraborty, A. Bhattarai, R. De, Synergistic and antagonistic effects in micellization of mixed surfactants, J. Mol. Liq. 368 (2022) 120678, https://doi.org/10.1016/J.MOLLIQ.2022.120678.
[23] T. Kobayashi, K. Mao, S.G. Wang, V.S.Y. Lin, M. Pruski, Molecular ordering of mixed surfactants in mesoporous silicas: a solid-state NMR study, Solid State Nucl. Magn. Reson. 39 (2011) 65–71, https://doi.org/10.1016/j.ssnmr.2011.02.001.
[24] A. Rehman, M.U. Nisa, M. Usman, Z. Ahmad, T.H. Bokhari, H.M.A.U. Rahman, A. Rasheed, L. Kiran, Application of cationic-nonionic surfactant based nanostructured dye carriers: mixed micellar solubilization, J. Mol. Liq. 326 (2021), https://doi.org/10.1016/j.molliq.2021.115345.
[25] B. Yang, K. Edler, C. Guo, H. Liu, Assembly of nonionic-anionic co-surfactants to template mesoporous silica vesicles with hierarchical structures, Microporous Mesoporous Mater. 131 (2010) 21–27, https://doi.org/10.1016/j.micromeso.2009.11.036.
[26] C. Liu, S. Wang, Z. Rong, X. Wang, G. Gu, W. Sun, Synthesis of structurally stable MCM-48 using mixed surfactants as co-template and adsorption of vitamin B12 on the mesoporous MCM-48, J. Non-Cryst. Solids 356 (2010) 1246–1251, https://doi.org/10.1016/j.jnoncrysol.2010.04.028.
[27] D. Chen, Z. Li, C. Yu, Y. Shi, Z. Zhang, B. Tu, D. Zhao, Nonionic block copolymer and anionic mixed surfactants directed synthesis of highly ordered mesoporous silica with bicontinuous cubic structure, Chem. Mater. 17 (2005) 3228–3234, https://doi.org/10.1021/cm050209h.
[28] E.B. Mubofu, J.E.G. Mdoe, G. Kinunda, The activity of invertase immobilized on cashew nut shell liquid-templated large pore silica hybrids, Catal. Sci. Technol. 1 (2011) 1423–1431, https://doi.org/10.1039/c1cy00033k.
[29] F.B. Hamad, E.B. Mubofu, Y.M.M. Makame, Wet oxidation of maleic acid by copper(ii) Schiff base catalysts prepared using cashew nut shell liquid templates, Catal. Sci. Technol. 1 (2011) 444–452, https://doi.org/10.1039/c1cy00001b.
[30] M. Andrew, E. Mubofu, Catalytic efficiency of palladium (II) supported on Castor oil based micelle templated silica for peroxide promoted catalytic wet oxidation of phenols, Int. Res. J. Pure Appl. Chem. 15 (2017) 1–12, https://doi.org/10.9734/IRJPAC/2017/36966.
[31] J. Mgaya, Trypsin immobilization on thiol functionalized mesoporous silicas prepared using Castor oil template, Tanzan. J. Sci. 46 (2020) 755–767, https://doi.org/10.4314/tjs.v46i3.16.
[32] S. Nyandoro, E. Elimbinz, Synthesis, characterisation and catalytic evaluation of Castor oil-templated mesoporous sulfated solid acid catalysts for esterification reaction, Tanzania, J. Eng. Technol. 41 (2022) 155–168, https://doi.org/10.52339/tjet.v41i4.875.
[33] N. Sunsandee, S. Phatanasri, U. Pancharoen, Separation of homogeneous palladium catalysts from pharmaceutical industry wastewater by using synergistic recovery phase via HFSLM system, Arab. J. Chem. 14 (2021) 103024, https://doi.org/10.1016/j.arabjc.2021.103024.
[34] E. Farnetti, R. Di Monte, J. Kašpar, Homogenous and Heterogenous Catalysis Inorganic and bio-inorganic chemistry 2 (6) (2009) 50–86.
[35] B. Salah, A.K. Ipadeola, A. Khan, Q. Lu, Y. Ibrahim, E.L. Darboe, A.M. Abdullah, K. Eid, Unveiling the electrochemical CO oxidation activity on support-free porous PdM (M = Fe, Co, Ni) foam-like nanocrystals over a wide pH range, Energy Convers. Manag. X 20 (2023) 100449, https://doi.org/10.1016/j.ecmx.2023.100449.
[36] A.K. Ipadeola, A.B. Haruna, A.M. Abdullah, M.F. Shibl, D. Ahmadaliev, K.I. Ozoemena, K. Eid, Electrocatalytic CO oxidation on porous ternary PdNiO-CeO2/carbon black nanocatalysts: effect of supports and electrolytes, Catal. Today 421 (2023) 114178, https://doi.org/10.1016/j.cattod.2023.114178.
[37] A.K. Ipadeola, A. Abdelgawad, B. Salah, A. Ghanem, M. Chitt, A.M. Abdullah, K. Eid, Self-standing foam-like Pd-based alloys nanostructures for efficient electrocatalytic ethanol oxidation, Int. J. Hydrogen Energy 48 (2023) 30354–30364, https://doi.org/10.1016/j.ijhydene.2023.04.149.
[38] S. Han, C. He, Q. Yun, M. Li, W. Chen, W. Cao, Q. Lu, Pd-based intermetallic nanocrystals: from precise synthesis to electrocatalytic applications in fuel cells, Coord. Chem. Rev. 445 (2021) 214085, https://doi.org/10.1016/j.ccr.2021.214085.
[39] S. Brunauer, P.H. Emmett, E. Teller, Adsorption of gases in multimolecular layers, J. Am. Chem. Soc. 60 (1938) 309–319, https://doi.org/10.1021/ja01269a023.
[40] E.P. Barrett, L.G. Joyner, P.P. Halenda, The determination of pore volume and area distributions in porous substances. I. Computations from nitrogen isotherms, J. Am. Chem. Soc. 73 (1951) 373–380, https://doi.org/10.1021/ja01145a126.
[41] K. Sing, The use of nitrogen adsorption for the characterisation of porous materials, Colloids Surfaces A Physicochem. Eng. Asp. 187–188 (2001) 3–9, https://doi.org/10.1016/S0927-7757(01)00612-4.
[42] M. Kruk, M. Jaroniec, Gas adsorption characterization of ordered organic-inorganic nanocomposite materials, Chem. Mater. 13 (2001) 3169–3183, https://doi.org/10.1021/cm0101069.
[43] S. Siles-Quesada, C.M.A. Parlett, A.C. Lamb, J.C. Manayil, Y. Liu, J. Mensah, H. Arandiyan, K. Wilson, A.F. Lee, Synthesis and catalytic advantage of a hierarchical ordered macroporous KIT-6 silica, Mater. Today Chem. 30 (2023) 101574, https://doi.org/10.1016/j.mtchem.2023.101574.
[44] F.B. Hamad, E.B. Mubofu, Y.M.M. Makame, Wet oxidation of maleic acid by copper(ii) Schiff base catalysts prepared using cashew nut shell liquid templates, Catal. Sci. Technol. 1 (2011) 444, https://doi.org/10.1039/c1cy00001b.
[45] E. Elimbinzi, S.S. Nyandoro, E.B. Mubofu, A. Osatiashtiani, J.C. Manayil, M.A. Isaacs, A.F. Lee, K. Wilson, Synthesis of amine functionalized mesoporous silicas templated by Castor oil for transesterification, MRS Adv 3 (2018) 2261–2269, https://doi.org/10.1557/adv.2018.347.
[46] L. Bayne, R.V. Ulijn, P.J. Halling, Effect of pore size on the performance of immobilised enzymes, Chem. Soc. Rev. 42 (2013) 9000–9010, https://doi.org/10.1039/c3cs60270b.
[47] Z. Ji, H. Wang, S. Canossa, S. Wuttke, O.M. Yaghi, Pore chemistry of metal–organic frameworks, Adv. Funct. Mater. 30 (2020) 1–24, https://doi.org/10.1002/adfm.202000238.
[48] P.-C. Kuo, Z.-X. Lin, T.-Y. Wu, C.-H. Hsu, H.-P. Lin, T.-S. Wu, Effects of morphology and pore size of mesoporous silicas on the efficiency of an immobilized enzyme. https://doi.org/10.1039/d1ra01358k, 2021.
[49] B. Bai, Q. Qiao, Y. Li, Y. Peng, J. Li, Effect of pore size in mesoporous MnO_2 prepared by KIT-6 aged at different temperatures on ethanol catalytic oxidation, Cuihua Xuebao/Chinese J. Catal. 39 (2018) 630–638, https://doi.org/10.1016/S1872-2067(18)63036-0.

[50] Y. Ma, G. Nagy, M. Siebenbürger, R. Kaur, K.M. Dooley, B. Bharti, Adsorption and catalytic activity of gold nanoparticles in mesoporous silica: effect of pore size and dispersion salinity, J. Phys. Chem. C 126 (2022) 2531–2541, https://doi.org/10.1021/acs.jpcc.1c09573.
[51] N.N.A. Mohamed Abdul Ghani, M.A. Saeed, I.H. Hashim, Thermoluminescence (TL) response of silica nanoparticles subjected to 50 Gy gamma irradiation, Malaysian J. Fundam. Appl. Sci. 13 (2017) 178–180, https://doi.org/10.11113/mjfas.v13n3.593.
[52] H. Zhang, C. Tang, C. Sun, L. Qi, F. Gao, L. Dong, Y. Chen, Direct synthesis, characterization and catalytic performance of bimetallic Fe-Mo-SBA-15 materials in selective catalytic reduction of NO with NH_3, Microporous Mesoporous Mater. 151 (2012) 44–55, https://doi.org/10.1016/j.micromeso.2011.11.018.